



# Broadband and top-flat mid-infrared supercontinuum generation with 3.52 W time-averaged power in a ZBLAN fiber directly pumped by a 2- $\mu\text{m}$ mode-locked fiber laser and amplifier

Jacek Swiderski<sup>1</sup> · Maria Michalska<sup>1</sup> · Pawel Grzes<sup>1</sup>

Received: 22 April 2018 / Accepted: 29 June 2018 / Published online: 3 July 2018  
© The Author(s) 2018

## Abstract

Supercontinuum generation from 1.87 to 4.03  $\mu\text{m}$  in a ZBLAN fiber is reported. A home-made passively mode-locked thulium-doped fiber laser and amplifier, providing 21.4-ps pulses at 81 MHz is used as a pump. The continuum output power is 3.52 W, of which 1.45 and 0.88 W corresponds to wavelengths longer than 3 and 3.5  $\mu\text{m}$ , respectively. A spectrum flatness of 2 dB over a bandwidth of 1710 nm, from 2.02 to 3.73  $\mu\text{m}$ , is also reported. This represents, to our knowledge, the best power conversion in the mid-infrared region and the best spectral flatness for high power supercontinuum generation in ZBLAN fibers directly pumped by 2- $\mu\text{m}$  CW mode-locked fiber lasers and amplifiers.

## 1 Introduction

High power supercontinuum (SC) generation with a broad spectral bandwidth in the mid-infrared (mid-IR) has recently attracted concern of many researchers. Such light sources can find applications in a lot of important areas, like stand-off detection [1], directional countermeasure [2], and medicine [3, 4]. For these applications, the magnitude of bandwidth, spectral flatness as well as the level of output power together with efficient power distribution towards the mid-IR are very important factors.

In principle, an SC can be generated by the use of an optical fiber with high nonlinearity and high peak power pulses. When mid-IR spectral region is concerned, soft glass fibers, including tellurite [5, 6], fluoride [1, 7–12] and chalcogenide [13, 14] fibers can be adopted as nonlinear media. However, among all soft glass fibers, only heavy metal fluoride fibers, including fluorozirconate (ZBLAN) [15–19] and fluoroindate ( $\text{InF}_3$ ) [20, 21] are technologically mature to be used for multi Watt level SC generation. Because they exhibit a zero-dispersion wavelength (ZDW) within the range of  $\sim 1.5$ – $1.9$   $\mu\text{m}$  they can be effectively pumped in

the anomalous dispersion region, which facilitates efficient continuum extension towards longer wavelengths. To this aim, thulium-doped fiber lasers and amplifiers (TDFL&As), providing high power, efficient and diffraction-limited output beam over a wide tuning range spread from  $\sim 1.9$  to 2.1  $\mu\text{m}$  can be used. When such pump light sources are employed, the whole SC system becomes relatively compact and stable compared with the ones utilizing, e.g., optical parametric oscillators (OPO) and amplifiers (OPA) [22].

Different types of pulsed thulium-doped fiber-based laser systems, such as mode-locked [18, 19], Q-switched and mode-locked [8, 23] as well as gain-switched and mode-locked [24, 25] providing femtosecond [7] and picosecond [23, 25] pulses, have been already proposed to pump fluoride fibers. In particular, CW model-locked fiber lasers followed by a cascade of amplifiers delivering optical pulses with pulse widths in the picoseconds range allow scaling output SC power to over 10 W, while being relatively easy in realization. This laser configuration is becoming increasingly important to address demands for pump sources for high-power mid-IR SC generation.

In 2013 Yang et al. reported a mid-IR SC extending from 1.9 to 3.9  $\mu\text{m}$  with an average output power of 7.11 W generated out of a ZBLAN fiber pumped by a 1.96  $\mu\text{m}$  master oscillator power amplifier (MOPA) system [15]. The SC power for wavelengths longer than 2.5  $\mu\text{m}$  was 3.52 W with a power ratio of 49.5% with respect to the total SC power. A year later, the group presented all-fiber integrated SC generation in a ZBLAN fiber with a spectrum extending from

✉ Jacek Swiderski  
jacek.swiderski@wat.edu.pl

<sup>1</sup> Institute of Optoelectronics, Military University of Technology, 2 Urbanowicza Street, 00-908 Warsaw, Poland

~ 1.9 to 4.3  $\mu\text{m}$  [16]. The output average power was 13 W, of which 52.69% corresponded to wavelengths beyond 2.5  $\mu\text{m}$ . In 2014 Liu et al. reported an SC with an output power of up to 21.8 W and a spectrum spanning from 1.9 to beyond 3.8  $\mu\text{m}$  generated in a ZBLAN fiber pumped by a mode-locked TDFL&A operating at ~ 1.93  $\mu\text{m}$  [17]. Soon after that, the same group demonstrated a record 24.3 W SC generation in a single-mode ZBLAN fiber pumped by a 2- $\mu\text{m}$  TDFA with a spectrum spanning from 1.9 to 3.3  $\mu\text{m}$  [18]. More recently, a 10-W-level SC with a spectrum extending from ~ 1.9 to 4.1  $\mu\text{m}$ , generated out of a fluorozirconate fiber pumped by a 1.95  $\mu\text{m}$  MOPA system with a SESAM mode-locked TDFL, was also reported by Zheng et al [19].

Despite the remarkably high power and/or broad output spectrum achieved, these works share similar limitations in the context of spectral flatness and/or efficient power distribution in the mid-IR spectral region. This results either from the limited peak power of pump pulses or limitation of ZBLAN fibers used as nonlinear media. Furthermore, all the reports concern the case when an SC is generated in a two-step process. The spectrum of pump signal is first initially broadened, typically up to ~ 2.4  $\mu\text{m}$ , in a TDFA or a piece of silica single-mode fiber (SMF) where pump pulses, as a result of modulation instability (MI), are broken into a series of solitons with durations in the femtosecond range. In the next step, the generated solitons are launched into a fluoride fiber and undergo further spectral broadening towards the mid-IR, mainly as a result of Raman-induced scattering [12].

In this paper, we report SC generation in a step-index ZBLAN fiber directly pumped by a home-built 1994.3 nm fiber-based picosecond MOPA system. The output time-averaged SC power was measured to be 3.52 W. The continuum power conversion efficiency for wavelengths beyond 3  $\mu\text{m}$  and 2-dB spectral flatness bandwidth are 1.45 W (41% of total output power) and 1710 nm, respectively. This presents, to the best of our knowledge, an increase in both spectral flatness and efficiency of power distribution compared to previously reported SC sources pumped by CW mode-locked TDFL&As.

## 2 Experimental setup

The experimental arrangement of the 2- $\mu\text{m}$  mode-locked fiber laser and amplifier system followed by a section for mid-IR SC generation is illustrated in Fig. 1. The pump pulse train is firstly amplified in a two-stage Tm-doped fiber power amplifier and then coupled directly (without initial broadening of pump pulses) into a single-mode ZBLAN fiber to stimulate SC generation.

The master oscillator has a linear cavity, composed of a 25-cm long step-index double-clad polarization-maintaining (PM) Tm-doped fiber (TDF) with clad absorption of

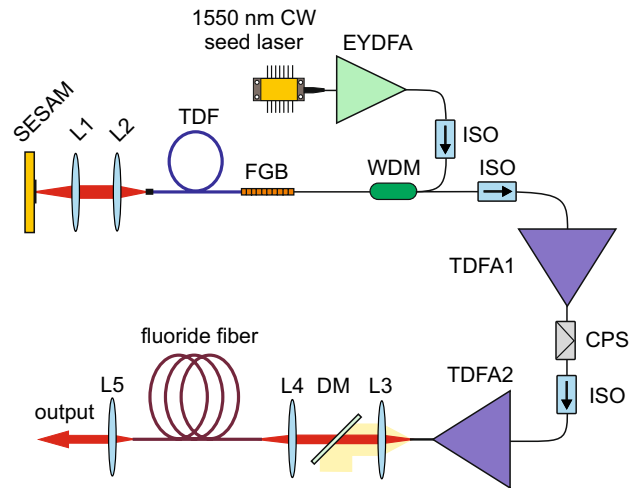


**Fig. 1** Schematic of the experimental setup for mid-IR SC generation. WDM—1550/2000 nm wavelength division multiplexer, TDFA—Tm-doped fiber amplifier, EYDFA—erbium:ytterbium-doped fiber amplifier, ISO—optical isolator, CPS—cladding pump stripper, DM—dichroic mirror, L1–L5—lenses, FBG—fiber Bragg grating, TDF—Tm-doped fiber

4.7 dB/m at 793 nm, a fiber Bragg grating (FBG) acting as the wavelength selecting component and a semiconductor saturable absorber mirror (SESAM) soldered on a gold plated Cu-cylinder. The cavity has an overall optical path length of 1.85 m corresponding to a fundamental repetition rate of 81 MHz. The gain fiber has a core diameter of 10  $\mu\text{m}$  and a numerical aperture (NA) of 0.15. One end of the active fiber is spliced to the FBG with 90% reflectivity at a center wavelength of 1994.5 nm and a full-width at half-maximum (FWHM) of 1.4 nm, which is used for narrowing pulse spectrum to achieve tens of picoseconds pulse width. The other TDF end is cleaved at an angle of 8° to avoid parasitic lasing. The SESAM, used in the experiment to initiate and maintain mode-locking (ML) operation of the laser, has a high reflectivity ( $R > 60\%$ ) from 1880 to 2090 nm, a modulation depth of 20%, non-saturable loss of 36%, relaxation time of 10 ps, and saturation fluence of 35  $\mu\text{J}/\text{cm}^2$ . It is coupled with the angle-cleaved TDF end through two AR-coated aspheric lenses with the same effective focal length of 5.95 mm. The active fiber is backward in-core pumped by a home-made 1.25 W continuous wave (CW) 1550-nm pump unit via a 1550/2000 nm high power fused wavelength division multiplexer (WDM) coupler, providing over 90% of pump coupling efficiency. No attempt was made to balance the intracavity dispersion.

The output fiber end of the 1550/2000 nm WDM, after optical isolation, is spliced to the first Tm-doped fiber amplifier (T DFA1). The 3-m long active fiber has the same parameters as the one used in the oscillator. A multimode pump combiner with a signal feedthrough is employed to deliver pump light to the Tm fiber from two 790-nm 4.5-W laser diodes with

105/125  $\mu\text{m}$  fiber pigtailed (0.22 NA). Following the TDF, a cladding pump stripper (CPS) is used to strip the unabsorbed pump light and protect the optical isolator (ISO).

The TDFA1 output, after stripping the unabsorbed pump power and optical isolation, is fusion spliced to the final Tm-doped fiber amplifier (marked as TDFA2), built with the use of large mode area double-clad TDF with a core/clad diameter of 25/250  $\mu\text{m}$ , NAs of 0.08/0.46 and clad absorption specified as 9.5 dB/m at 793 nm. It is pumped by two fiber-pigtailed multimode 790-nm 30-W laser diodes, light of which is delivered by a  $(2 + 1) \times 1$  pump combiner. The active fiber is wrapped on an aluminum drum with a diameter of less than 15 cm to ensure cooling and good beam quality. Its output end is angle cleaved to avoid unwanted reflections. At the output of the pump system, a dichroic mirror (HR@0.79  $\mu\text{m}$ , HT@2  $\mu\text{m}$ , 45° coated) is used to filter the unabsorbed 790-nm pump light.

Finally, the amplified 2- $\mu\text{m}$  pulse train is launched into a 12-m long step-index fluorozirconate fiber by a telescope (lenses L3 and L4), allowing for a launch efficiency of over 60%. The nonlinear fiber has a core/clad diameter of 6.8/125  $\mu\text{m}$ , an NA of 0.23 and a cut-off wavelength of 2.04  $\mu\text{m}$ . The ZBLAN fiber was customized to a small core area and a relatively large NA to ensure good confinement of a pump beam in a core region. The losses within the wavelength range of 1.3–3.75  $\mu\text{m}$  were below 0.05 and 0.2 dB/m at 4  $\mu\text{m}$ . The fiber ZDW was measured to be 1603 nm [10]. Both ends of the fluoride fiber are angle cleaved to avoid unwanted damage caused by Fresnel reflections. To prevent thermal damage of the nonlinear fiber, it is wrapped on an aluminum cylinder with machined spiral grooves. The output from the fluoride fiber is also collimated by means of a single  $\text{CaF}_2$  lens (L5).

The power was measured with a thermal power meter (Ophir, LaserStar), the 2- $\mu\text{m}$  pump laser spectrum fluence was measured by an optical spectrum analyzer (Yokogawa, AQ6375) whereas the SC spectrum was monitored by a grating monochromator (Princeton Instruments, SP-2300) equipped with a thermo-electrically cooled HgCdTe detector (Vigo System S.A.). To avoid the effects of high-order diffraction peaks of the grating, appropriate long-pass filters were placed in front of the detection system. Pulse waveforms were recorded by a 12.5-GHz InGaAs photodetector (Electro-Optics Technology, ET-5000) together with a 6-GHz bandwidth, 25-GSa/s oscilloscope (Tektronix, DSA 70604) as well as an autocorrelator (Femtochrome Research Inc., FR-103WS).

### 3 Results and discussion

The Tm-doped fiber oscillator, after a proper adjustment of the SESAM provided stable CW mode-locked pulses with a repetition rate of 81 MHz, corresponding to the

optical cavity length. Like in case of soliton fiber lasers, it was observed that the laser went through several working regimes occurring sequentially with a continuous increase in the pump power. The operating-regime distribution of the oscillator and the corresponding output power versus the pump power as well as oscilloscope traces illustrating the regimes are shown in Figs. 2 and 3, respectively.

The oscillator started to operate at CW regime after reaching the threshold launched pump power of 288 mW. Increasing the pump power from 302–321 mW leads to Q-switching and mode-locking (Fig. 3a), originating from a relatively high modulation depth of the SESAM. Once the launch pump power was higher than 321 mW, irregular mode-locking was observed. In this mode of operation doublet pulses of high amplitude, spaced by 1.1 ns, were generated (Fig. 3b). For pump power over 340 mW, a stable, self-starting CW mode locking was achieved (Fig. 3c) and maintained until ~435 mW. When the higher pump power was applied the laser started to operate unstably.

The maximum average output power for stable ML was measured to be 17 mW. The laser operated at a central wavelength of 1994.3 nm with a 3 dB width of 0.27 nm (inset in Fig. 2). The slope efficiency of the laser in a ML regime with respect to the launched pump power is 1.5%, which is typical for this type of oscillators. The duration of output pulses could not be measured by our autocorrelator because of their low peak power. Therefore, the pulse width was measured after the final amplifier.

As a next step, the pulses from the output of the seed oscillator were boosted in the two-stage amplifier. The

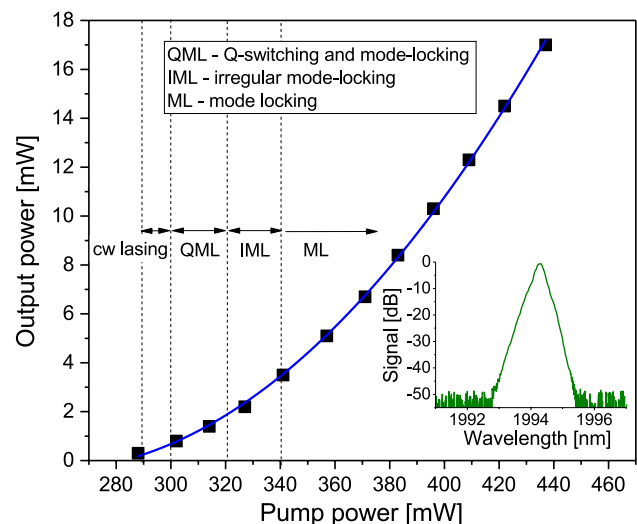


**Fig. 2** The Tm-doped fiber oscillator output power versus launched pumped power with marked different mode-locking regimes distribution. QML—Q-switching and mode-locking, IML—irregular mode-locking, ML—stable CW mode-locking. Inset, output spectrum of ML pulses

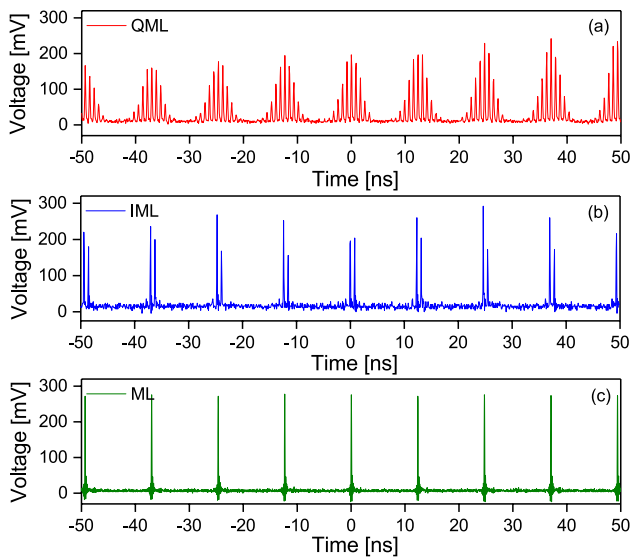


**Fig. 3** Measured output pulse train in Q-switching and mode-locking **a** irregular mode-locking **b** and stable CW mode-locking **c** regimes

TDFA1 provided the maximum average output power of 1.92 W at an absorbed 790-nm pump power of 9.3 W, with a slope efficiency of 29%. Except for a small signal of amplified spontaneous emission (ASE), no obviously nonlinear effects were observed in the optical spectrum. The noise-to-signal ratio (SNR) was measured to be 49 dB. The final power amplifier TDFA2 was assembled in the similar way as the TDFA1. A 3.4-m long large mode area Tm-doped fiber with a core/clad diameter of 25/250  $\mu\text{m}$  was employed mainly to avoid nonlinear effects occurring during amplification of short optical pulses. The average power of incident pulse train, launched into the gain fiber, was 0.9 W. The TDFA2 delivered an average output power of 23.68 W for 58.75 W of absorbed pump power, which corresponds to a slope efficiency of 44% (Fig. 4). As can be seen, the output power increased almost linearly with the rise of pump power with no roll-off of the curve. The maximum pulse energy was calculated to be 292.3 nJ. Figure 5 shows the spectrum of the amplified ML pulses. The center wavelength locates at 1994.3 nm and the spectrum bandwidth (FWHM) is 0.34 nm measured at the maximum average output power. The output spectrum was moderately broadened when compared with the oscillator, probably due to self-phase modulation (SPM).

The output spectrum was also clear without any artifacts coming from nonlinear effects (upper inset in Fig. 4). The ASE signal in the amplifier is about 47.5 dB down compared with the amplified signal, showing that the MOPA system operates with very low-intensity noise. It is worth adding that the system was tested for several hours a day over 2 weeks without any significant degradation of output parameters. The lower inset in Fig. 4 presents the short-term output power stability under laboratory conditions,

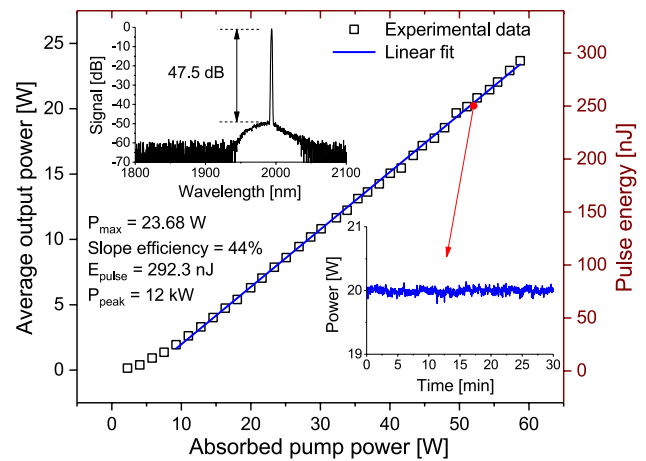


**Fig. 4** Average output power and pulse energy of the TDFA2 as a function of absorbed 790-nm pump power. Upper inset, spectrum of amplified pulses recorded over a 300-nm bandwidth scale. Lower inset, short-term output power stability measured over 30 min

monitored over 30 min. Once the stable ML operation was achieved the laser system delivered a stable pulse train with power fluctuations within 3%, which is mainly caused by fluctuations in pump power of the TDFA2.

The autocorrelation trace of the amplified 2- $\mu\text{m}$  pulses at the maximum average output power is shown in Fig. 6. The FWHM of the autocorrelation trace was 33 ps. If a sech<sup>2</sup> pulse profile is assumed, the pulse width is 21.4 ps. Consequently, the time-bandwidth product, when combined with the 0.34 nm spectral bandwidth, was calculated to be 0.548, which is slightly higher than the theoretical transform limit. With better dispersion management in the laser cavity, by reducing the length of a passive anomalous-dispersion fiber and inserting a piece of a normal dispersion fiber at 2- $\mu\text{m}$  wavelength, shorter ML pulses are expected. The maximum

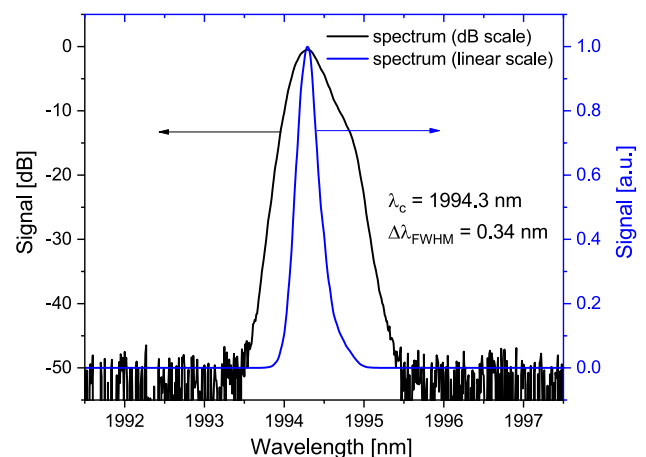


**Fig. 5** Spectrum of amplified 2- $\mu\text{m}$  pulses at the maximum average output power

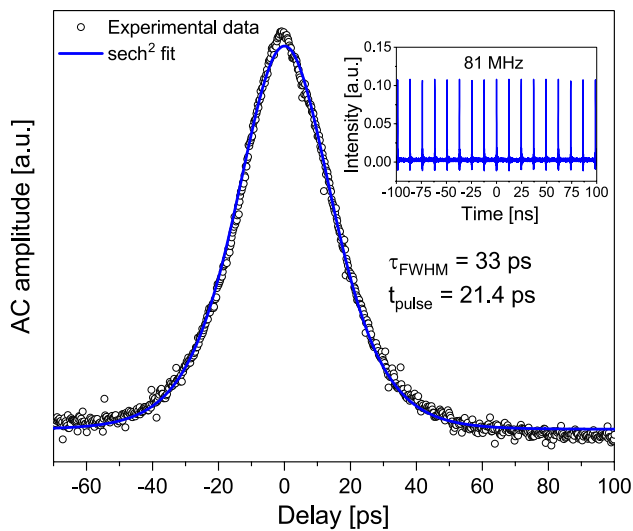


**Fig. 6** Autocorrelation trace of the amplified 2- $\mu\text{m}$  pulses at the maximum average output power (circles) and its squared hyperbolic secant fit (solid curve). The inset shows the stable pulse train with a repetition rate of 81 MHz

peak-power of the amplified pulses was 12 kW and currently this value is limited by available pump power. Further scaling the pulse peak power is ongoing.

In the final part of the study, an SC generation in the ZBLAN fiber pumped by the 2- $\mu\text{m}$  MOPA system, characterized above, was examined. The evolution of the SC output spectrum for different output SC power levels is shown in Fig. 7. The spectra were recorded after passing through a long-pass filter with a cut-off edge at a wavelength of 1.85  $\mu\text{m}$ , and they were corrected for the detector and grating responsivities.

Increasing the output SC power, the long-wavelength cut-off was gradually extended towards the red wavelengths, which is typical for pumping a nonlinear fiber deep in the anomalous dispersion region [26]. When the output power was  $\sim 1$  W, the SC spectrum extended to 3.6  $\mu\text{m}$ . It can be also noticed that the higher output power the higher spectral flatness can be achieved. When the output power reached 3.52 W (for an incident pump power of 10.5 W), the spectrum spread from 1.87 to 4.03  $\mu\text{m}$ . The spectral range was considered according to the noise level of the detection system. The dip at  $\sim 2.7$   $\mu\text{m}$  corresponds to  $\text{OH}^-$  ion absorption in the detection system. The power ratio of SC for wavelengths longer than 2.5, 3 and 3.5  $\mu\text{m}$  is over 66% (2.34 W), 41% (1.45 W) and 25% (0.88 W), respectively. The spectrum has a flatness of 5 dB at the wavelength range of 2.01–3.84  $\mu\text{m}$  and less than 2 dB (assuming the dip corresponding to water absorption is neglected) at the wavelength range of 2.02–3.73  $\mu\text{m}$  (1710 nm bandwidth). The infrared edge of the spectrum resulted from the loss edge of fluoride glass as well as limited peak power of pump pulses.

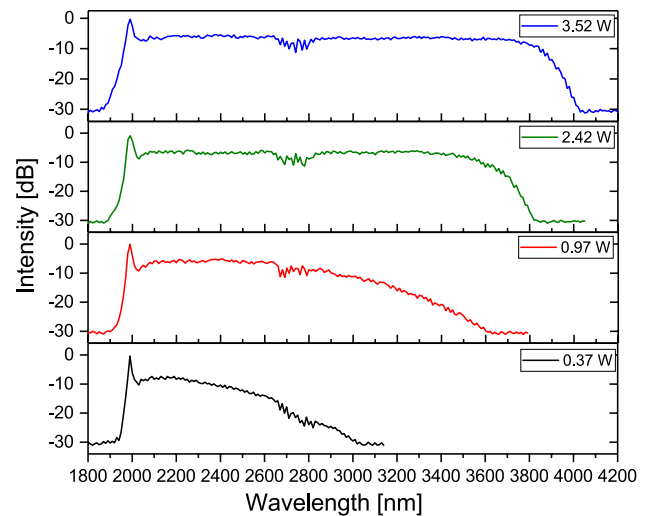


**Fig. 7** Mid-IR SC spectra recorded at different output power levels

The observation of the SC evolution at shorter wavelengths ( $< 1.9$   $\mu\text{m}$ ) was not carried out, mainly because of limitations with our detection system. Further power scaling-up was limited by the damage to the ZBLAN fiber output facet. Both the SC power conversion towards the red wavelengths and flatness of output spectrum are better than the recent results [15–19]. It also shows that applying a SESAM mode-locked TDFL&A delivering pulses with tens of picoseconds and a low loss ZBLAN fiber it is possible to develop a high power and super flat mid-IR SC source with very good power distribution towards the mid-IR spectral region. Consequently such sources can meet the demands imposed by many applications, like for instance those pointed out in the Introduction.

## 4 Conclusions

In conclusion, an all-fiber CW mode-locked fiber laser and two-stage fiber amplifier system operating a wavelength of 1994.3 nm is reported. The maximum average power of amplified pulse train, generated at a fundamental repetition rate of 81 MHz, was 23.68 W, yielding pulse energies of 292.3 nJ. The pulse width was measured to be 21.4 ps. The peak power of the output pulses, estimated by assuming a  $\text{sech}^2$  shape, is 12 kW. Using this laser source as a pump for a step-index single-mode ZBLAN fiber, a supercontinuum spectrum covering the whole 2–4  $\mu\text{m}$  wavelength region with 3.52 W time-averaged power was demonstrated. The SC power for wavelengths longer than 2.5, 3 and 3.5  $\mu\text{m}$  is 2.34, 1.45 and 0.88 W, with a power ratio of 66, 41 and 25% (determined with respect to the total SC output power), respectively. A spectral flatness of 2 dB over a bandwidth of 1710 nm is also presented. To the best of our knowledge, this

represents the best power conversion in the mid-IR spectral region and the best spectral flatness of SC generated out of a ZBLAN fiber directly pumped by 2- $\mu\text{m}$  CW mode-locked fiber lasers and amplifiers. The mid-IR SC average output power can be further increased if higher pump power and a special cooling of nonlinear fiber facets are provided.

**Acknowledgements** This research leading to these results was mainly supported by the National Science Centre, Poland (Grant no. UMO-2014/13/B/ST7/00442). Pawel Grzes would like to acknowledge financial support (scholarship) from the Polish National Science Centre. Special acknowledgments are given to Marcin Mamajek and Jan Karczewski from the Institute of Optoelectronics MUT for discussions and technical support.

**Open Access** This article is distributed under the terms of the Creative Commons Attribution 4.0 International License (<http://creativecommons.org/licenses/by/4.0/>), which permits unrestricted use, distribution, and reproduction in any medium, provided you give appropriate credit to the original author(s) and the source, provide a link to the Creative Commons license, and indicate if changes were made.

## References

- M. Kumar, M.N. Islam, F.L. Terry, M.J. Freeman, A. Chan, M. Neelakandan, T. Manzur, Stand-off detection of solid targets with diffuse reflection spectroscopy using a high-power mid-infrared supercontinuum source. *Appl. Opt.* **51**, 2794–2807 (2012)
- H.H.P.T. Bekman, J.C. van den Heuvel, F.J.M. van Putten, R. Schleijsen, Development of a mid-infrared laser for study of infrared countermeasures techniques. *Proc. SPIE* **5615**, 27–38 (2004)
- J. Nallala, G.R. Lloyd, C. Kendall, N.A. Shepherd, H. Barr, N. Stone, Identification of GI cancers utilizing rapid mid-infrared spectral imaging. *Proc. SPIE* **9703**, 970303 (2016)
- A. Seddon, Mid-infrared (IR)—a hot topic: the potential for using mid-IR light for non-invasive early detection of skin cancer in vivo. *Phys. Status Solidi B* **250**, 1020–1027 (2013)
- R. Thapa, D. Rhonehouse, D. Nguyen, K. Wiersma, C. Smith, J. Zong, A. Chavez-Pirson, Mid-IR supercontinuum generation in ultra-low loss, dispersion-zero shifted tellurite glass fiber with extended coverage beyond 4.5  $\mu\text{m}$ . *Proc. SPIE* **8898**, 889808 (2013)
- S. Kedenburg, C. Strutynski, B. Kibler, P. Froidevaux, F. Desevedavy, G. Gadret, J.-C. Jules, T. Steinle, F. Morz, A. Steinmann, H. Giessen, F. Smektala, High repetition rate mid-infrared supercontinuum generation from 1.3 to 5.3  $\mu\text{m}$  in robust step-index tellurite fibers. *J. Opt. Soc. Am. B* **34**, 601–607 (2017)
- J. Luo, B. Sun, J. Liu, Z. Yan, N. Li, E.L. Tan, Q. Wang, X. Yu, Mid-IR supercontinuum pumped by femtosecond pulses from thulium doped all-fiber amplifier. *Opt. Express* **24**, 13939–13945 (2016)
- C. Kneis, B. Donelan, I. Manek-Honninger, T. Robin, B. Cadier, M. Eichhorn, C. Kieleck, High-peak-power single-oscillator actively Q-switched mode-locked Tm<sup>3+</sup>-doped fiber laser and its application for high-average output power mid-IR supercontinuum generation in a ZBLAN fiber. *Opt. Lett.* **41**, 2545–2548 (2016)
- W.-Q. Yang, B. Zhang, J. Hou, K. Yin, Z.-J. Liu, A novel 2- $\mu\text{m}$  pulsed fiber laser based on a supercontinuum source and its application to mid-infrared supercontinuum generation. *Chin. Phys. B* **23**, 054208 (2014)
- M. Michalska, P. Hlubina, J. Swiderski, Mid-infrared supercontinuum generation to  $\sim 4.7 \mu\text{m}$  in a ZBLAN fiber pumped by an optical parametric generator. *IEEE Photon. J.* **9**, 3200207 (2017)
- K. Yin, B. Zhang, L. Yang, J. Hou, 15.2 W spectrally flat all-fiber supercontinuum laser source with  $> 1 \text{ W}$  power beyond 3.8  $\mu\text{m}$ . *Opt. Lett.* **42**, 2334–2337 (2017)
- C. Xia, Z. Xu, M.N. Islam, F.L. Terry, M.J. Freeman, A. Zakel, J. Mauricio, 10.5 W time-averaged power mid-IR supercontinuum generation extending beyond 4  $\mu\text{m}$  with direct pulse pattern modulation. *IEEE J. Sel. Top. Quantum Electron.* **15**, 422–434 (2009)
- R.R. Gattass, L.B. Shaw, V. Nguyen, P. Pureza, I.D. Aggarwal, J.S. Sanghera, All-fiber chalcogenide based mid-infrared supercontinuum source. *Opt. Fiber Technol.* **18**, 345–348 (2012)
- C.R. Petersen, U. Moller, I. Kubat, B. Zhou, S. Dupont, J. Ramsay, T. Benson, S. Sujecki, N. Abdel-Moneim, Z. Tang, D. Furniss, A. Seddon, O. Bang, Mid-infrared supercontinuum covering the 1.4–13.3  $\mu\text{m}$  molecular fingerprint region using ultra-high NA chalcogenide step-index fibre. *Nat. Photonics* **8**, 830–834 (2014)
- W. Yang, B. Zhang, K. Yin, X. Zhou, J. Hou, High power all fiber mid-IR supercontinuum generation in a ZBLAN fiber pumped by a 2  $\mu\text{m}$  MOPA system. *Opt. Express* **21**, 19732–19742 (2013)
- W. Yang, B. Zhang, G. Xue, K. Yin, J. Hou, Thirteen watt all-fiber mid-infrared supercontinuum generation in a single mode ZBLAN fiber pumped by a 2  $\mu\text{m}$  MOPA system. *Opt. Lett.* **39**, 1849–1852 (2014)
- K. Liu, J. Liu, H. Shi, F. Tan, P. Wang, High power mid-infrared supercontinuum generation in a single-mode ZBLAN fiber with up to 21.8 W average output power. *Opt. Express* **22**, 24384–24391 (2014)
- K. Liu, J. Liu, H. Shi, F. Tan, P. Wang, “24.3 W mid-infrared supercontinuum generation from a single-mode ZBLAN fiber pumped by thulium-doped fiber amplifier,” in *Advanced Solid State Lasers, OSA Technical Digest* (online) (Optical Society of America, 2014), paper AM3A.6
- Z. Zheng, D. Ouyang, J. Zhao, M. Liu, S. Ruan, P. Yan, J. Wang, Scaling all-fiber mid-infrared supercontinuum up to 10 W-level based on thermal-spliced silica fiber and ZBLAN fiber. *Photon. Res.* **4**, 135–139 (2016)
- M. Michalska, P. Grzes, P. Hlubina, J. Swiderski, Mid-infrared supercontinuum generation in a fluoroindate fiber with 1.4 W time-averaged power. *Laser Phys. Lett.* **15**, 045101 (2018)
- J. Swiderski, F. Theberge, M. Michalska, P. Mathieu, D. Vincent, High average power supercontinuum generation in a fluoroindate fibre. *Laser Phys. Lett.* **11**, 015106 (2014)
- M. Michalska, J. Mikołajczyk, J. Wojtas, J. Swiderski, Mid-infrared, super-flat, supercontinuum generation covering the 2–5  $\mu\text{m}$  spectral band using a fluoroindate fibre pumped with picosecond pulses. *Sci. Rep.* **6**, 39138 (2016)
- C. Kneis, B. Donelan, A. Berrou, I. Manek-Honninger, B. Cadier, F. Joulain, M. Poulain, I. Manek-Honninger, M. Eichhorn, C. Kieleck, 4.5 W mid-infrared supercontinuum generation in a ZBLAN fiber pumped by a Q-switched mode-locked Tm<sup>3+</sup>-doped fiber laser. *Proc. SPIE* **9342**, 93420B (2015)
- W.Q. Yang, B. Zhang, J. Hou, R. Xiao, R. Song, Z.J. Liu, Gain-switched and mode-locked Tm/Ho-codoped 2  $\mu\text{m}$  fiber laser for mid-IR supercontinuum generation in a Tm-doped fiber amplifier. *Laser Phys. Lett.* **10**, 045106 (2013)
- P. Grzes, J. Swiderski, Gain-switched 2- $\mu\text{m}$  fiber laser system providing kilowatt peak-power mode-locked resembling pulses and its application to supercontinuum generation in fluoride fibers. *IEEE Photon. J.* **10**, 1500408 (2018)
- J.M. Dudley, R. Taylor (eds.), *Supercontinuum Generation in Optical Fibers* (Cambridge University Press, Cambridge, 2010)